BULLETIN OF THE POLISH ACADEMY OF SCIENCES
TECHNICAL SCIENCES, Vol. 73(5), 2025, Article number: e155035
DOI: 10.24425/bpasts.2025.155035

Research on a method for capturing bullets with limited deformation for forensic comparative examination

Dawid PACEK[1]*, **Przemyslaw BADUROWICZ**[1], and **Roman GIELETA**[2]

[1] Military Institute of Armament Technology, ul. Wyszyńskiego 7, 05-220 Zielonka, Poland
[2] Military University of Technology, ul. Kaliskiego 2, 00-908, Warszawa, Poland

Abstract. There are currently no solutions that could be effectively used for stopping a wide range of non-full metal jacket bullets without deformation. The paper presents research on the elaboration of a novel solution in the form of a material system combining composite and fluid. It contains a demonstration of the results proving its effectiveness and an analysis of the solutions of bullet traps currently used in forensic laboratories, as well as the system based on a composite structure proposed for the current needs. The experimental tests and the numerical simulations of bullet impact into water, with a nominal velocity, are described. The critical value of impact velocity V_{cr} (which does not cause deformation of the bullet) was found numerically. The composite reducing bullet velocity to V_{cr} was prepared and tested. With the use of the composite and plasticine, a monolithic hollow point 9 mm GECO Action Extreme bullet was decelerated and slowly stopped in such a manner as not to cause bullet deformation. The proposed method could therefore be used to capture non-full metal jacket bullets in a form facilitating the determination of whether the given weapon was used to fire a projectile of the same type as the one found at the crime scene.

Keywords: forensic tests; bullet catcher; ballistic test; numerical simulation.

1. INTRODUCTION

Research work described in the paper was performed as part of the project: Laboratory stand for stopping high-energy projectiles. Since recognition of traces on bullets is necessary for weapon identification (Fig. 1), the main goal of the project is to develop a laboratory stand to be used in forensic applications to stop high-energy bullets without significant deformations.

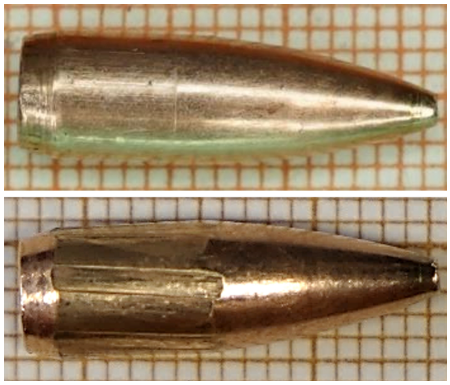

Fig. 1. Traces on a bullet investigated in forensic laboratories

In forensic tests of weapons, microscopic comparative studies of bullets fired from high-energy weapons, e.g., rifles, are performed. To maintain the necessary quality of barrel traces, such bullets need to be fired with full energy from the weapon and then captured, causing as insignificant damage as possible. Most of the hunting bullets are designed to undergo plastic deformation once they hit the animal's body. Deformed bullets are of limited or no traceability if the deformation extends to a cylindrical guide part on which barrel marks are left. Currently, there is no effective technology for capturing such penetrators. As crimes can be committed using diverse types of ammunition, e.g., hunting, civilian, or military, there are various needs in forensic laboratories.

Methods used nowadays in forensic laboratories, such as bullet catchers with finely fragmented solid materials [1, 2], stands with low density solid layers [3], and water bullet traps [4–6], enable stopping some types of bullets whose deformation is limited enough to permit their use as reference sample to compare ballistic traces found on the crime scene. However, they are not useful in the case of every type of projectile. The results of stopping two types of bullets in water with extremely different degrees of deformation are shown in Fig. 2.

The left side depicts the undeformed full metal jacket bullets (FMJ), and the right side exemplifies the fragmented high-energy bullets, susceptible to deformation, which could not be used in forensic laboratories.

The research aims to elaborate methods that allow deceleration and slowly stop bullets susceptible to deformation so that they remain completely or sufficiently intact. If both the cylindrical and the ogival part of the projectile are not deformed, it should be understood that the projectile was stopped without

*e-mail: pacekd@witu.mil.pl

Manuscript submitted 2025-05-03, revised 2025-06-12, initially accepted for publication 2025-06-27, published in August 2025.

© 2025 The Author(s). This is an open access article under the CC BY license (http://creativecommons.org/licenses/by/4.0/)

(a) (b)

Fig. 2. Exemplary bullets stopped in water: (a) full metal jacket bullets; (b) fragments of non-full metal jacket bullets

deformation. If the cylindrical part, where the barrel has left its traces, is left intact, while deformation has occurred in the ogival section, the bullet can be considered to have undergone limited deformation.

The intended solution is to use the combination of composite and fluid, for example, water (Fig. 3). Water itself causes excessive deformations in the case of bullet impact with a nominal velocity, while an individual composite would probably be too expensive and too long to be used in laboratory conditions. First, it is crucial to find the value of the impact velocity into water, V_{cr}, corresponding to acceptable deformations of bullets. Then, it is necessary to find an appropriate composite structure that could reduce impact velocity $V_{i\,\mathrm{nom}}$ to a value of velocity equal to or below V_{cr}.

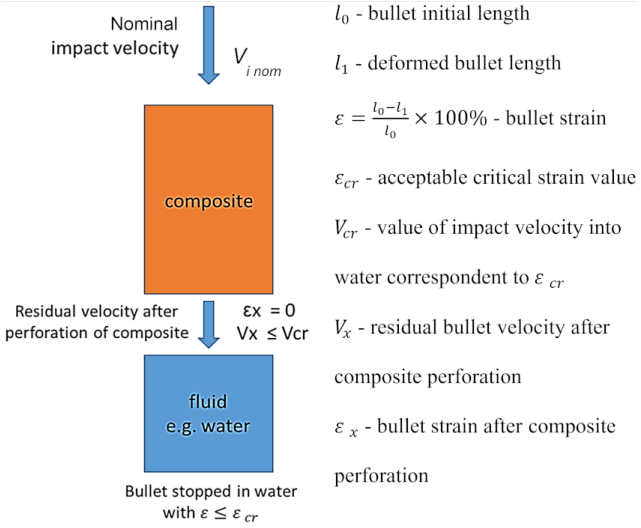

Fig. 3. A scheme of a material set for catching bullets susceptible to deformation

The paper describes the results of the ballistic tests, SHPB tests (split Hopkinson pressure bar), and a numerical simulation for a monolithic hollow point 9 mm GECO Action Extreme bullet. The research was divided into the following stages:

1. First, bullet impact into water, with nominal velocity, was investigated (experimental tests and numerical simulations were performed).
2. Then, the behavior of a bullet after impact with the water, with velocity below nominal, was analyzed using the Autodyn software for dynamic analyses. At this stage, a critical value of impact velocity V_{cr} was found.
3. In the next step, a composite which reduces $V_{i\,\mathrm{nom}}$ to V_{cr} was developed.
4. Finally, experimental tests of bullet impacts into a material set of composite and plasticine were conducted. The plasticine has a 50% greater density than water. From previously conducted research, it is also known that it causes bigger deformations to projectiles than water. Therefore, it can be assumed that if a bullet were stopped in plasticine without deformation, it would certainly be trapped in water also without deformation.

2. LITERATURE REVIEW

Bullet catchers and soft recovery methods are used for research of projectile or forensic purposes. The literature contains a few reports, papers, patents, and utility models related to this problem. The studies are mainly focused on FMJ small arms bullets or artillery projectiles. There is no literature on the soft catching of small arms bullets susceptible to deformation. The current paper aims to fill this gap and therefore presents the research concerning this area not described in previous works.

This method can be used for a pistol as well as for both intermediate and rifle bullets. It is included, for example, in the report [1] describing the structure of a bullet catcher and an experimental procedure for catching bullets without deformation. The bullet recovery device consists of cartons stacked one after the other. The cartons are filled with insulation – vermiculite with styrene foam mixed with sawdust at a ratio of 50%:50%. The bullet catcher stops a 7.62 mm FMJ rifle bullet (not specified in the text, but from [1, Fig. 4] you can assume that it is 7.62×54 R or 7.62×51 mm) as well as a 20 mm and a 30 mm bullet without significant deformations (the types of projectiles are not specified in the text and this is also not clear from [1, Figs. 5 and 6]). The report [7] presents research on the flight characteristics of the M855 NATO ball ammunition. For this purpose, a soft recovery method is required, with the recovery device using gelatin blocks.

Soft recovery methods can also be used for catching explosively formed penetrators (EFPs) and artillery projectiles. The report [2] describes a device for the safe recovery of explosively formed penetrators. The device is used for capturing the bullet for metallurgical analysis and for validating high-rate constitutive material models. The paper [8] describes a soft recovery system, which is a device for stopping bullets without damaging them. This device is necessary to verify the shock-resistant requirements of microelectronics and electro-optic sensors in smart munitions. The recovery system consists of a long tube attached to a gun barrel, which has the same diameter as the bullet and contains diaphragms causing high pressure in front of the projectile and, hence, stops it. The report [4] describes a

large caliber bullet soft recovery system using water, with the apparatus employing a water scoop mounted onto the bullet. The projectile is exposed to increasing depths of water because this whole assembly is angled slightly. The deceleration length is 60 meters. This system is designed for bullet calibers: 105 mm, 155 mm, and 203 mm. The known patents concerning bullet traps are used mostly for firearm discharging, firearm testing, and intercepting bullets without significant deformations. The patent [3] describes a bullet trap used for verifying the discharging of firearms. The bullet catcher consists of a rectangular housing with one open wall, containing a material that absorbs the kinetic energy of the bullet. These materials can be layers of different density rubbers and of different metals. The patent [5] describes a water bullet trap, in which water is the medium absorbing the kinetic energy of the projectile. The bullet catcher is used for firearm testing, and the water is contained in a closed tank with a window for a weapon barrel. This design limits its spillage during a shot. The patent [6] shows a hydrodynamic bullet trap in which bullets are intercepted in water flowing at high speed in the same direction as the bullets. The flowing water destabilizes the bullets, which shortens the bullet stopping distance. The advantages of this solution, according to the invention, are as follows: no projectiles remain in the water since projectiles are intercepted from the flowing water, there is a relatively short bullet stopping distance, and less water is required to fill the bullet trap than in the case of other common water bullet traps. The patent [9] describes a set of technical aids for a bullet catcher, which consists of a weapon mount and a bullet trap. The bullet trap is a pipe with material absorbing the kinetic energy of the bullet. The set is designed, for further research, to intercept bullets without significant deformations. Another invention [10] relates to a polymeric ballistic material containing polyethylene of high molecular weight and high density, which is used to stop bullets. It can be used in shooting ranges as well as to protect not only personnel but also vehicles, airplanes, and other installations exposed to ballistic impact. In [11], the composition and preparation of a polymer or polymer blend of ballistic material capable of absorbing incoming small arms bullets are described. The materials are sufficiently elastic so as not to shatter when the bullet is halted. The material can be used in shooting ranges or to protect vehicles and other infrastructure. The patent in [12] relates to apparatus and methods for measuring the terminal ballistics of projectiles, focusing on measuring a wound cavity. Bullets are stopped by a test tube with special media with characteristics similar to animal tissues. The invention mainly concerns the preparation and packaging of absorbent material. Another invention presents a high-velocity bullet take-back device used for testing the velocity attenuation rule of the projectiles. The main parts of the device are a take-back box and a velocity measurement frame. Different soft catching media, allowing bullets to be intercepted without deformations, can easily be replaced in the take-back box [13].

The utility model described in [14] is a portable gun speed measuring bullet collection device containing a closed box for catching the projectiles, a speed measuring device, and a plurality of industrial silicon rubber plates for intercepting the bullets.

3. MATERIALS AND METHODS

3.1. Experimental tests of bullet impact into water

Experimental tests were conducted using a water bullet catcher for vertical shooting (Fig. 4). The dimensions of the water container were: 2 m height and 0.48 m width and depth. The behavior of a monolithic hollow point 9 mm GECO Action Extreme

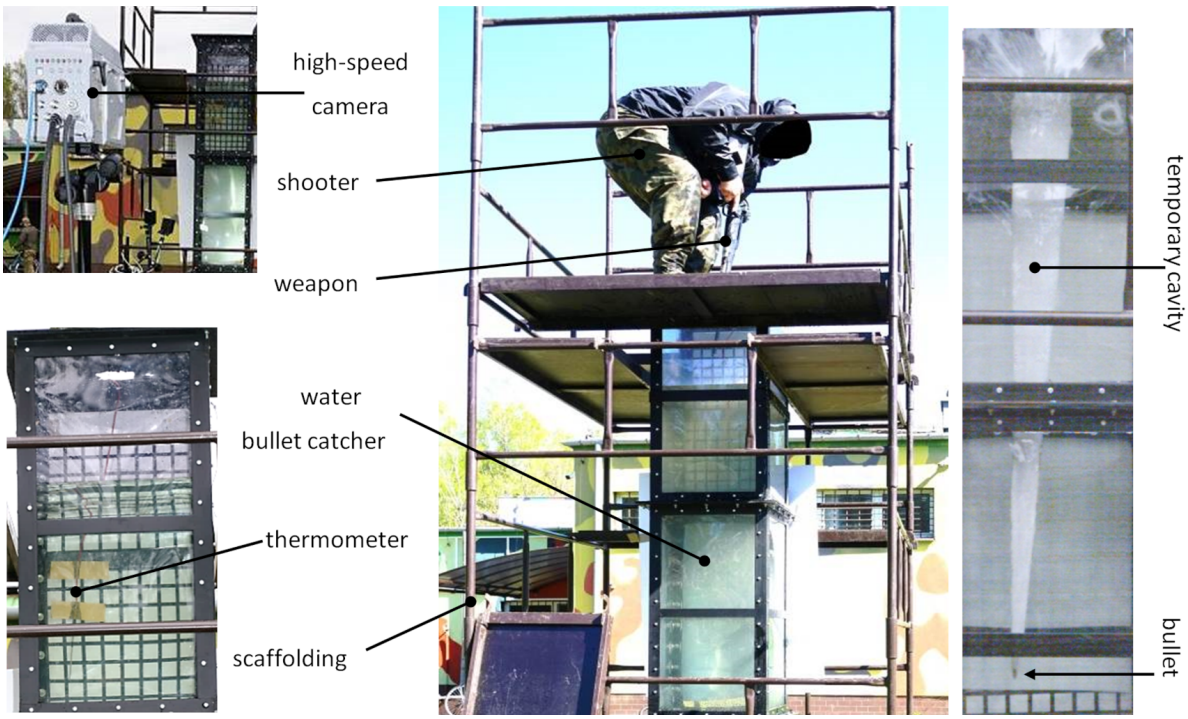

Fig. 4. Vertical water bullet catcher – research on energy threshold causing projectile deformation

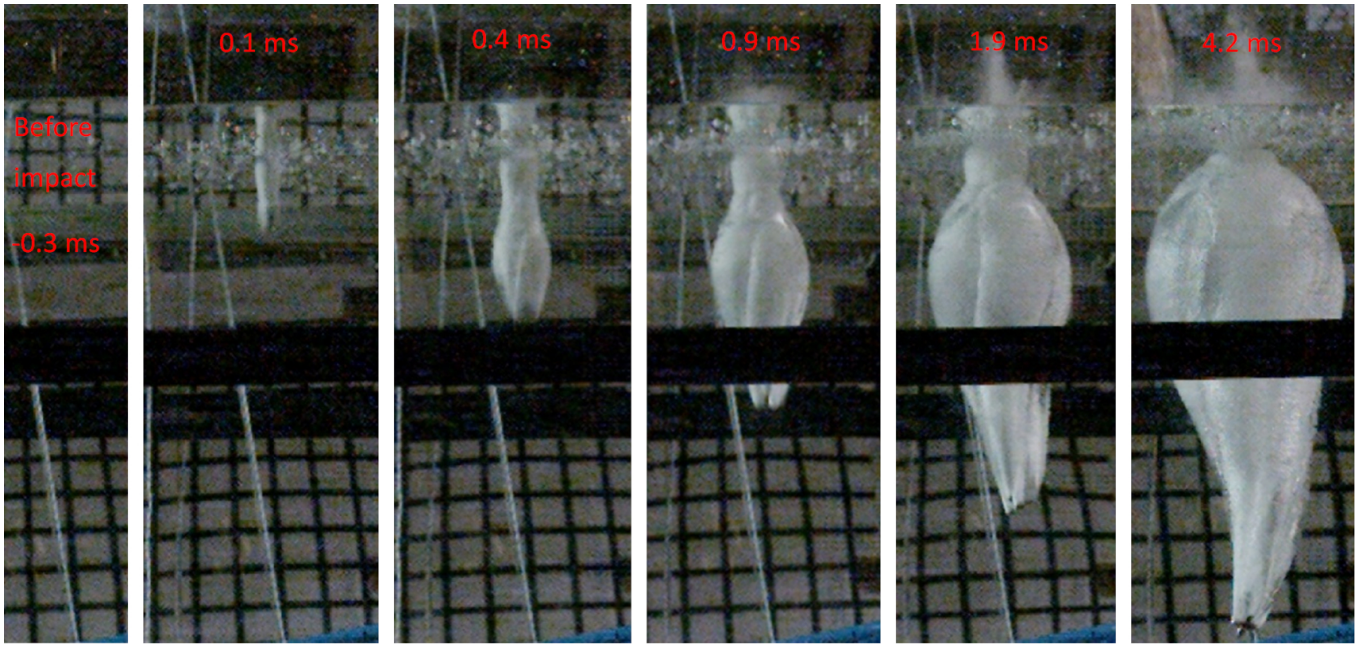

Fig. 5. High-speed camera images of projectile impact into water

bullet (mass – 7 g; nominal muzzle velocity: 370 m/s) was investigated.

The shots were fired perpendicular to the water surface to prevent bouncing off the bullets. The bullets were observed during flights using the Photron Fastcam SA-Z 2100K high-speed camera (Fig. 5). The speed recording of the camera was set at 20 000 fps (frames per second) and resolution 1024 × 1024 pixels. After the test, the deformed bullets were removed from the bullet trap and their characteristic dimensions were measured.

3.2. Numerical simulation of bullet impact into water

3.2.1. Numerical model of bullet

The numerical simulations were performed in Ansys Autodyn. To describe the elastic-plastic behavior of a 9 mm GECO Action Extreme bullet, the Johnson-Cook strength model was used. This model expresses the equivalent yield stress as a function of plastic strain ε, strain rate $\dot{\varepsilon}$, and temperature T, and is expressed with the following formula [15]:

$$\sigma_y = [A + B\varepsilon^n] \times [1 + C \ln \dot{\varepsilon}^*] \times [1 - T^{*m}], \tag{1}$$

which includes five material constants: A – static yield stress, B – strain hardening coefficient, n – strain hardening exponent, C – strain rate coefficient, m – thermal softening exponent and where

$$\dot{\varepsilon}^* = \frac{\dot{\varepsilon}}{\dot{\varepsilon}_0} \tag{2}$$

is dimensionless plastic strain rate, $\dot{\varepsilon}_0$ – reference rate of plastic deformation (1 s^{-1}), and where

$$T^* = \frac{T - T_r}{T_m - T_r} \tag{3}$$

is homologous temperature (dimensionless value of temperature), T_r – room temperature, T_m – melting temperature.

Damage to the material was described using the Johnson-Cook failure model related to the accumulation of plastic strain

$$D = \sum \frac{\Delta\varepsilon}{\varepsilon^f}, \tag{4}$$

$$\varepsilon^f = \left[D_1 + D_2 e^{D_3 \sigma^*}\right] \times [1 + D_4 \ln(\dot{\varepsilon}^*)] \times [1 + D_5 T^*], \tag{5}$$

where $\Delta\varepsilon$ – increment of the effective plastic strain, ε_f – equivalent plastic strain to failure, $\sigma* = p/\sigma_e$ – pressure/stress measureless dependence, p – pressure, σ_e – equivalent stress, D_1, D_2, D_3, D_4, D_5 – material constants.

The Johnson-Cook failure model is an "immediate failure model", which means that when a component fails, its stiffness and strength are automatically reduced to zero. Failure occurs when the failure parameter D reaches a value of 1. The bullet was discretized by 2326 unstructured tetrahedron elements, which were set as average nodal pressure (ANP). A real bullet, a CAD model, and an MES model are presented in Fig. 6.

Material parameters were adopted based on own previous papers [16–18], the literature [15, 19–21], and the Autodyn Material Database (Tables 1–3).

Not only does the numerical model require adopting parameters related to mathematical models, aimed at representing bullet behavior mechanics, but also those related to the environment in which the numerical simulation is performed (numerical method) [20, 21]. They include parameters related to contact between the parts of the model, allowable differences in the energy balance, or the removal (erosion) of finite elements whose deformations are significant enough to cause both a decrease in a time step and extension of the calculation time to an unacceptable extent. A triple erosion criterion was used in this

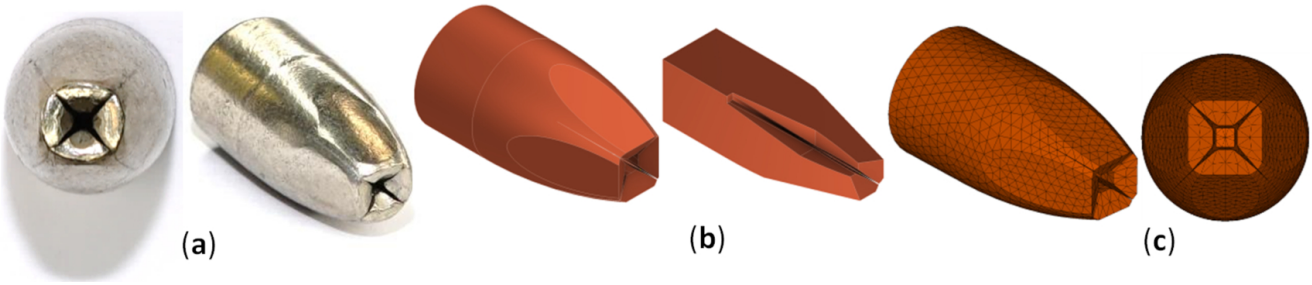

Fig. 6. 9×19 mm GECO Action Extreme bullet: (a) real bullet; (b) CAD model; (c) discretized model

Table 1
Material parameters of copper

Density ρ (g/cm^3)	Shear modulus G (GPa)	Melting temperature T_{melt} (K)	Bulk modulus K (GPa)	Specific heat (J/kgK)
8.96	46	1356	129	383
[15]	[1]AMD	[15]	AMD	[15], AMD

[1]AMD – Autodyn Material Database

Table 2
Strength model parameters used in numerical simulations [15]

Material	Johnson-Cook strength model				
	A, (GPa)	B, (GPa)	C	n	m
Copper	0.090	0.292	0.025	0.31	1.09

Table 3
Failure model parameters used in numerical simulations [15]

Material	Johnson-Cook failure model				
	D_1	D_2	D_3	D_4	D_5
Copper	0.54	4.89	3.03	0.014	1.12
Reference	[16]		[16]		[16]
	[17–19]	[17–19]	[17–19]	[17–19]	[17–19]

case: erosion strain set at 5.0; erosion timestep 2.0×10^{-6} ms, and erosion after element failure. Such parameters must be precisely selected to enable the conduct of the analysis as well as to maintain the 'physicality' of the phenomenon modeled. The discretization of the model adopted (both size and type of finite elements) also significantly influences numerical analyses. With growth in the number of finite elements (reduction in their size), more precise results may generally be expected; however, the calculation time is extended. Consequently, depending on the computing power possessed, a compromise is required.

The influence on the final result of the numerical simulation of the adopted material and numerical parameters, as well as on the division into finite elements, leads to the fact that even the adoption of credible and confirmed material data does not guarantee proper reflection of the phenomenon being modelled. Therefore, in the case of the numerical analyses conducted, it was decided that the numerical model of the bullet in the first step should be verified before performing the target simulations of the impact of the bullet into water.

3.2.1.1. Split Hopkinson pressure bar experimental tests

It was decided that the numerical model based on the comparison of the results of the experimental test in which the bullet would be subjected to a dynamic load within the scope, causing strong plastic strain, should be verified with a numerical simulation reflecting this study. It was assumed that the only element permanently deformed in the test would be the bullet. It should be possible to observe the deformation process, the duration of which should be short enough to recreate the experimental test in the software used for dynamic analyses.

In the last version, a split Hopkinson pressure bar (SHPB) stand was selected for dynamic tests of material properties (Fig. 7) [22–33]. The stand in the version intended for the presented studies was composed of a propelling system, a striker (SB) in the form of a cylinder with diameter $\varphi S = 20$ mm and length LS = 200 mm, incident (IB) and transmission (TB) steel bars arranged coaxially with respect to the striker ($\varphi = 25$ mm, $L = 2000$ m), a system for velocity measurement, measurement sensors, and a system for the recording and visualization of the sensor signals. A high-speed camera was also used in the test for precise observation of the bullet deformation process.

3.2.1.2. Split Hopkinson pressure bar simulation tests

Having obtained a satisfactory high degree of bullet deformation in the experimental test ($\varepsilon = \Delta l / l_0 = 38.55\%$), a numerical model reflecting the test was prepared (Fig. 8). The dimensions and masses of the bars, consistent with the experimental tests, as well as the velocity of the striker bar impact on the bullet, $V_i = 22.91$ m/s, were adopted. The material parameters for the bars were adopted based on the literature [15] and the Autodyn Material Database (Table 4).

Table 4
Steel bar strength model parameters used in simulations [15]

Material	Johnson-Cook strength model				
	A (GPa)	B (GPa)	C	n	m
Steel	0.350	0.275	0.022	0.36	1.00

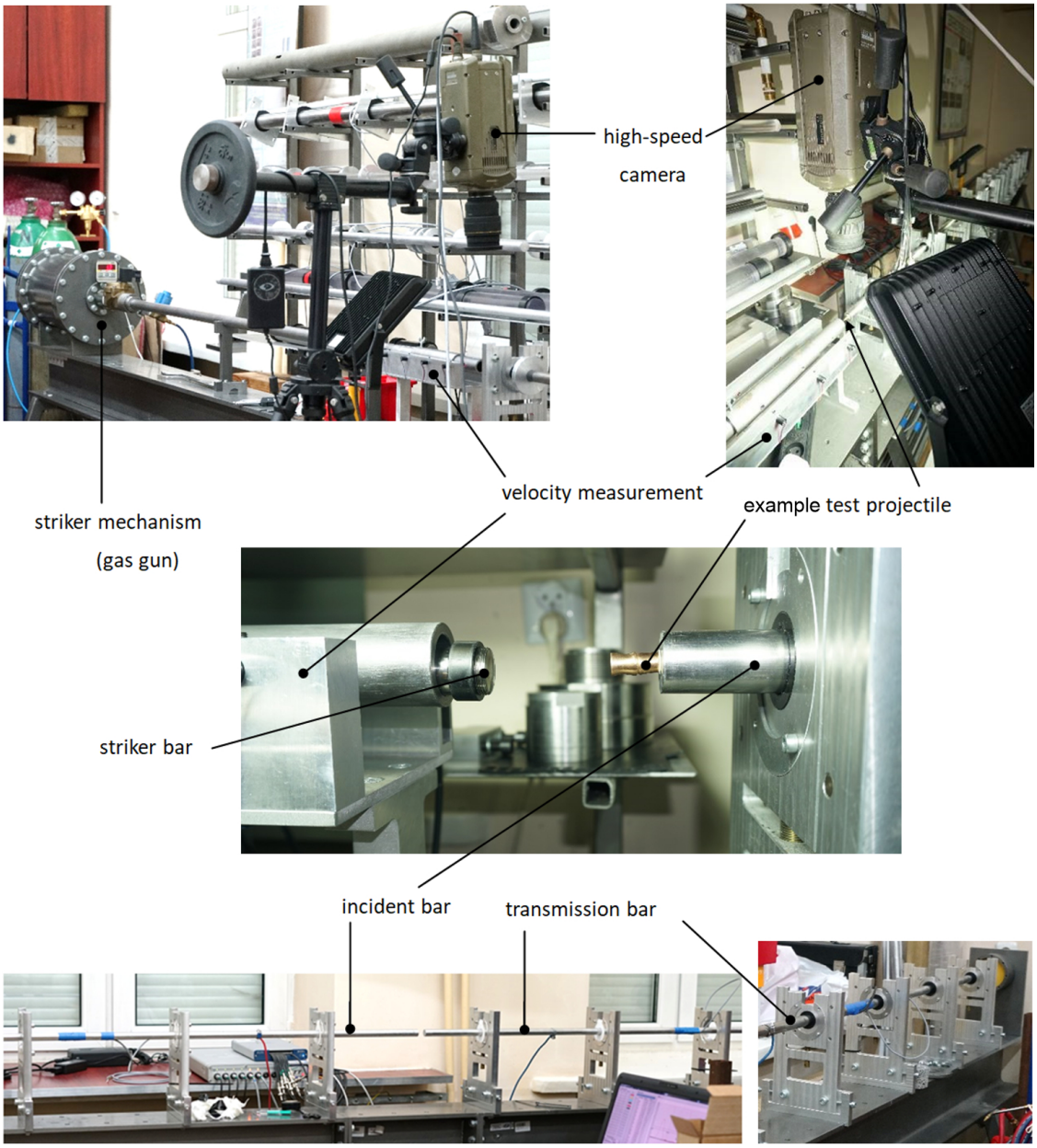

Fig. 7. Split Hopkinson Pressure Bar (SHPB) stand

3.2.2. Simulation of bullet impact into water – nominal impact velocity

A block of water with dimensions of $200 \times 200 \times 500$ mm was modeled. It was divided into 1 016 991 ($51 \times 51 \times 391$) elements with a size gradient towards the center (Fig. 9).

The Lagrange discretization formula was used for the bullet, while the Euler description was employed for the water block. Gravity was set in the direction of the projectile movement to reflect a vertical shot according to experimental tests. The model is symmetrical, and its quadrant was considered to reduce the computation time.

To describe the water, the "shock" equation of state was used. For most solids and many liquids over a wide pressure range, there is an empirical linear relationship between the speed of propagation of the shock wave U and the mass velocity of the medium behind the shock wave front u_p [34]

$$U = c_0 + s u_p \,, \tag{6}$$

where c_0, s – constants. Based on the above relationship, the following form of the equation of state is formulated [34]

$$p = p_H + \Gamma \rho \,(e - e_H) \,, \tag{7}$$

where it is assumed that the product of the Gruneisen Gamma Γ and density ρ is constant and

$$p_H = \frac{\rho_0 c_0^2 \mu (1+\mu)}{[1-(s-1)\mu]^2} \,, \tag{8}$$

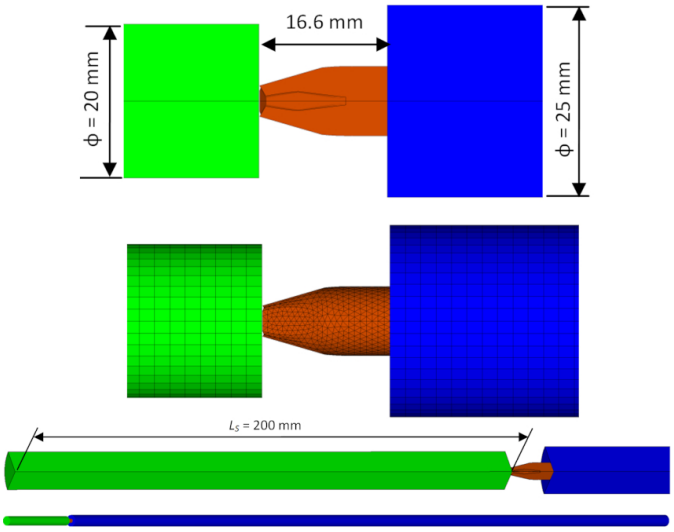

Fig. 8. A numerical model reflecting the tests performed on the SHPB stand

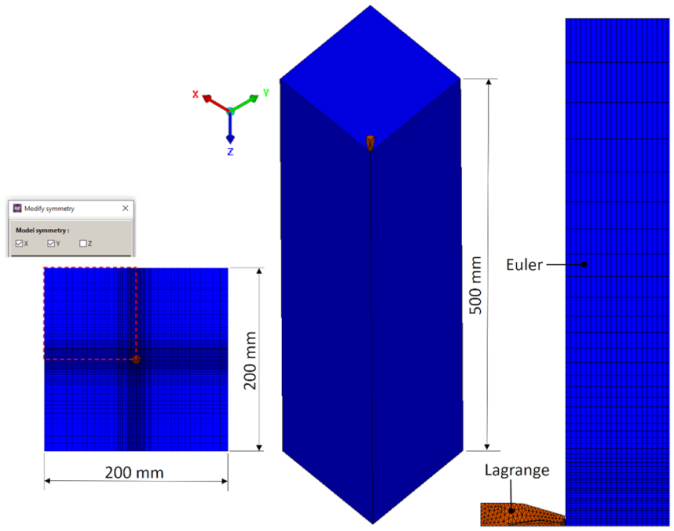

Fig. 9. Numerical model of a 9×19 mm Geco Action Ext. impact into water

$$e_H = \frac{1}{2}\frac{p_H}{\rho_0}\left(\frac{\mu}{1+\mu}\right), \tag{9}$$

where compression $\mu = (\rho/\rho_0) - 1$ and ρ_0 – initial density.

The material parameters of the water from Autodyn Material Database used in the numerical simulation are presented in Table 5.

Table 5
Material parameters of water

Density, ρ, (g/cm^3)	c_0, (m/s)	s
0.998	1647	1.921

First, a simulation of an impact into water at the velocity obtainable at the outlet of the barrel was performed, at the default surplus weight of the powder for a 9×19 mm Geco Action Extreme bullet. In the further part of the paper, this will be defined as the nominal velocity. According to the information provided by the producer, this velocity should be $V_0 = 400$ m/s. Based on the authors' tests, in the ballistic tunnel with the use of gates with photocells dedicated to the measurements of high velocities, a bullet velocity of $V_0 = 370$ m/s was obtained. This velocity was adopted as the nominal velocity for numerical calculations.

3.2.3. Simulation of bullet impact into water – decreased impact velocity

Having tested the correctness of the numerical model by comparing the simulation and the experimental results, an analysis of the behavior of bullets for impact velocities below a nominal value started. Ten impact velocities, from 50 to 350 m/s, were investigated. The aim was to find the critical value of the velocity – the highest possible velocity for which bullet deformation is acceptable. In this case, it was assumed that there should not be any deformations and $\varepsilon_{cr} = 0$.

3.3. A composite system for a bullet catcher

Having found that the critical value of the impact velocity V_{cr} is within a range of 100–150 m/s (Section 4.4), research on the development of a composite structure started. The following requirements for the material set were assumed:

- A need to reduce the impact velocity of the bullet from the nominal value (370 m/s) to 100 m/s or lower, and therefore absorbing minimum kinetic energy of 255 J.
- The bullet should not be deformed after perforation.
- The length of the whole structure should be shorter than 2 m.

Eventually, a composite structure with a length of 1.8 m, built from alternately placed high-strength and low-density layers, was developed. In connection with the planned patent proceedings, it is not possible to provide more detailed information about the composite.

4. RESULTS

4.1. Results of SHPB experimental tests

In the first system, the bullet was placed between the incident bar IB and the transmission bar TB; however, the striker impacted the IB bar. For the highest possible gas pressures of the propelling system, translated into SB bar impact velocity, relatively small deformations of a 9×19 mm monolithic copper GECO Action Extreme bullet were obtained. In order to obtain larger deformations of the bullet, its position in the testing system was changed, and it was placed at the front of the IB bar with its front part oriented in the direction of the striker. Thus, in this case, the SB bar impacted the bullet directly and as expected, larger deformations of the bullet were obtained. For an impact velocity $V_i = 22.1$ m/s, the length and the diameter of the deformed bullet were $l_1 = 10.2$ mm and $\varphi_1 = 11.42$ mm ($l_0 = 16.6$ mm and $\varphi_0 = 9.0$ mm), respectively. Selected moments of the bullet deformation process (impact of the striker into the bullet), in the form of frames recorded with the high-speed camera, are presented in Fig. 10.

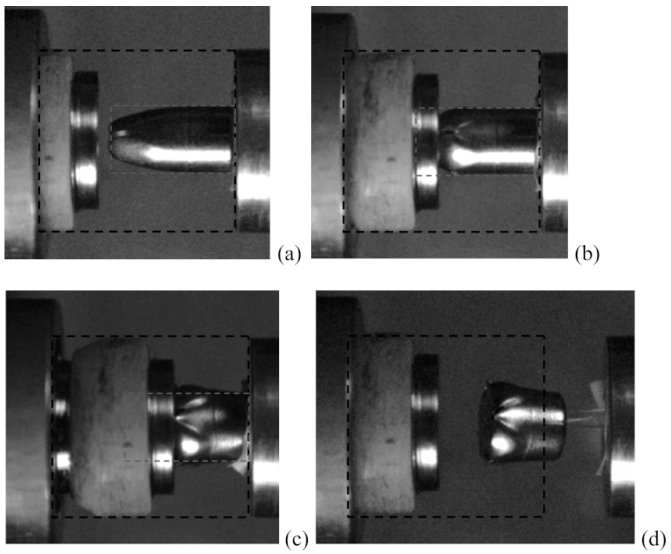

Fig. 10. Dynamic compression of 9 × 19 mm GECO Action Extreme bullet: (a) before striker impact, (b) first stage of compression of the ogival bullet part, (c) end of bullet compression, (d) bullet after the striker moves back

4.2. Results of SHPB simulation tests

Figure 11 presents the deformed bullets obtained after the impact of the striker both in the numerical simulation and the laboratory test. The differences in the length and diameter in the numerical simulation and the laboratory test were $\Delta l_1 = 0.87$ mm and $\Delta\varphi_1 = 0.21$ mm, respectively. A relatively low level of discrepancy in terms of the phenomenon (high plastic deformations, deformation velocity, occurrence of fractures in the material) was considered acceptable. It was decided to use the now validated numerical model of the bullet for further numerical analyses of the impact into water.

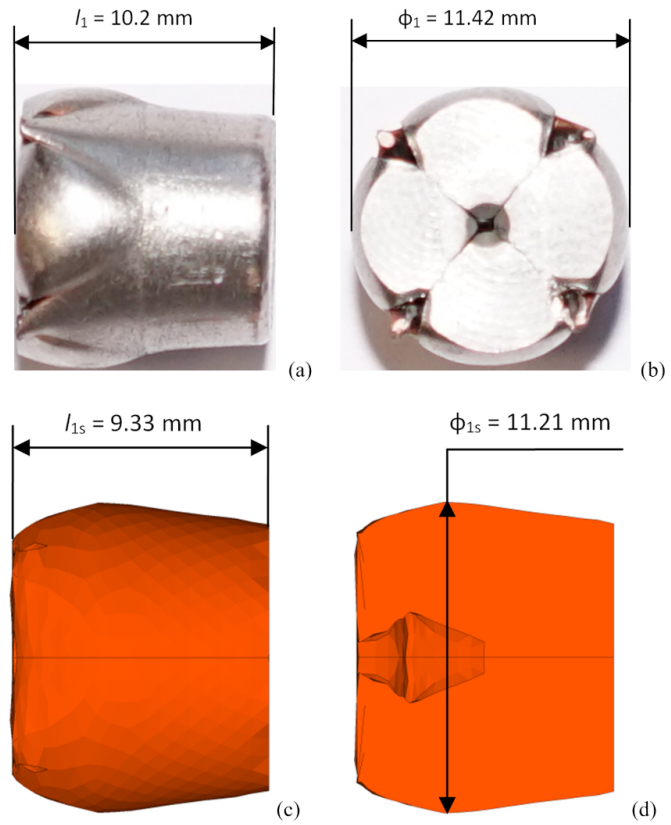

Fig. 11. A 9 × 19 mm Geco Action Extreme bullet after the striker impact (V_i = 22.1 m/s): (a) experimental test-side view, (b) experimental test-front view, (c) numerical simulation – side view, (d) numerical simulation – side cross-section view

4.3. Results of simulation of bullet impact into water – nominal impact velocity

A 9 × 19 mm Geco Action Extreme bullet is divided, in its front section, into four scraps with a space between them inside the bullet (Fig. 6). This space starts from the bullet tip and extends to approximately 2/3 of its length. During immersion of the bullet in a medium with relatively low density, such as soft tissues, plasticine, or water, the space is filled with the medium, and then, along with the pressure increase, bending in the outer direction to the axis of the bullet scraps occurs.

In the numerical simulation for impact velocity V_i = 370 m/s (Fig. 12), it is visible that full opening of the bullet occurs in

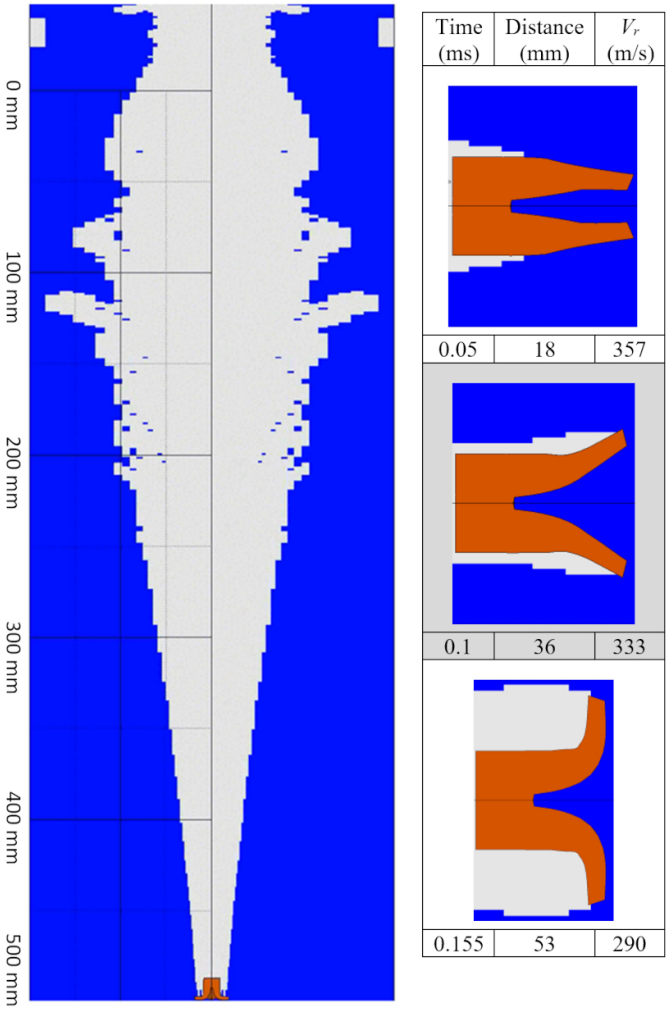

Fig. 12. Numerical simulation of bullet impact into water (V_i = 370 m/s) – bullet deformation

water up to a distance of about 53 mm. At 500 mm, however, the bullet is almost stopped as the residual velocity is only 3.5 m/s.

Based on the high-speed camera recordings, the course of changes in the velocity of the bullet in time was determined. The graph obtained along with an analogous curve from the Autodyn software designed for dynamic analyses is presented in Fig. 13.

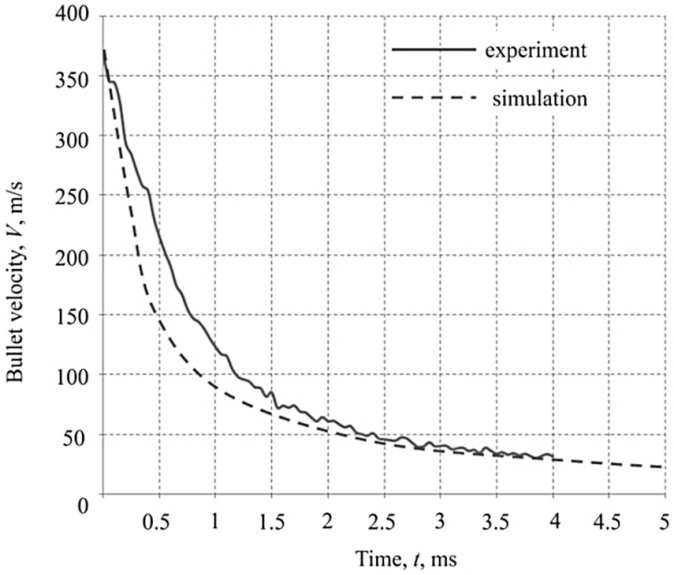

Fig. 13. Velocity changes over time – comparison of results for experiment and simulation

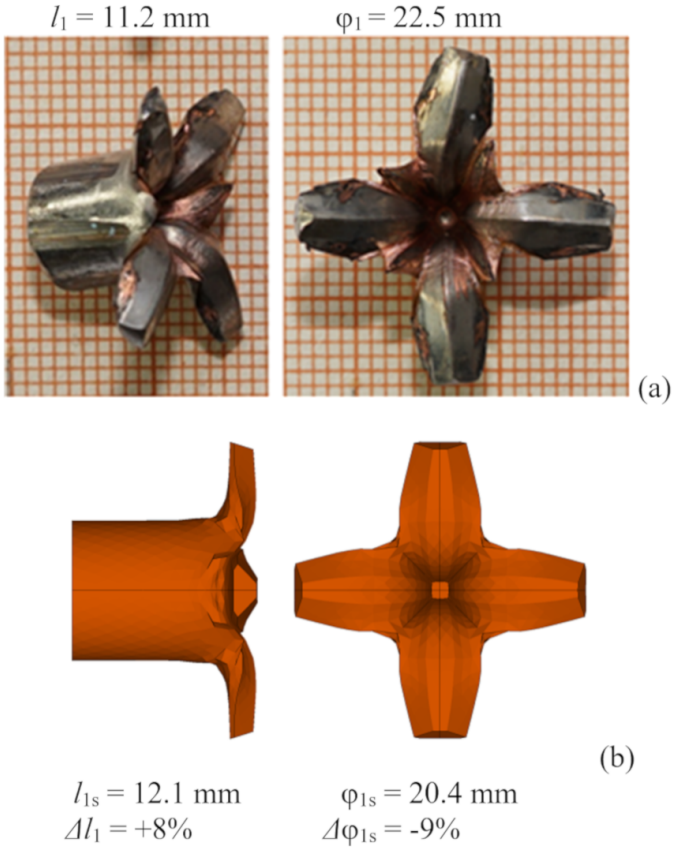

Fig. 14. Deformed bullet after impact into water: (a) laboratory ballistic test; (b) numerical simulation

The shape and course of both curves are similar. Up to 2.5 ms, there are some differences, as the velocity decrease rate is higher in the simulation, and after this period, both curves are convergent. Initial differences are related to the details of the deflection process of bullet flowering (expansion). Then, both plastic deformations and propagation of fractures in the material occur. This results in the fact that the reflection of this part of the experimental test in numerical analysis is especially difficult and burdened with a greater error. Considering the compliance of the plots in the further part of the paper, the influence of the initial differences needs to be considered negligible for the way the bullet decelerates. Apart from the comparison of the above-described curves, the final deformation of the bullet was adopted as the other criterion in the compliance assessment of the simulation and the experiment. Following the completion of the laboratory test and numerical analysis, the diameters and lengths of the deformed bullets were measured and compared (Fig. 14). Further, the general character and mechanisms of deformation were analyzed and compared. Comparing the deformations of bullets obtained with numerical investigation and experimental tests, the findings show a qualitative and quantitative similarity, which confirms the correctness of the methods applied and the stated assumptions. The dimensional differences are equal to 8–9%, which in the case of phenomena with such extensive plastic deformations and high strain rates is a satisfactory result. Having confirmed correct reflection of the deceleration process and deformation of a 9×19 mm Geco Action Extreme bullet in water, the model was selected for further parametric numerical analyses.

4.4. Results of simulation of bullet impact into water – decreased impact velocity

The final deformations for most of the impact velocities tested are presented in Fig. 15. No deformations are observed up to 100 m/s. As the next investigated impact velocity was 50 m/s greater, it should be stated that the critical value sought, V_{cr}, is within the range of 100 and 150 m/s. For further values of impact velocities, it is observed, as might be expected, that an increase in the final bullet diameter and a decrease in the final bullet length occur alongside an increase in impact velocity. Figure 16 presents the relationship between residual velocity and impact velocity for different distances in water.

For 50 mm, the relationship is approximately linear. For 100 mm, in the case of impact velocities greater than or equal to 250 m/s, all residual velocities are similar (in the range of 186–210 m/s). For distances of 200 mm and 400 mm, the extremum corresponding to an impact velocity equal to 250 m/s is observed. Up to this value, the residual velocity increases along with the impact velocity growth, while in the case of higher impact velocities, a residual velocity decrease occurs.

Figure 17 shows the dependence of velocity on distance for various impact velocities. In the case of the relationship of distance to time for different impact velocities (Fig. 18), with an

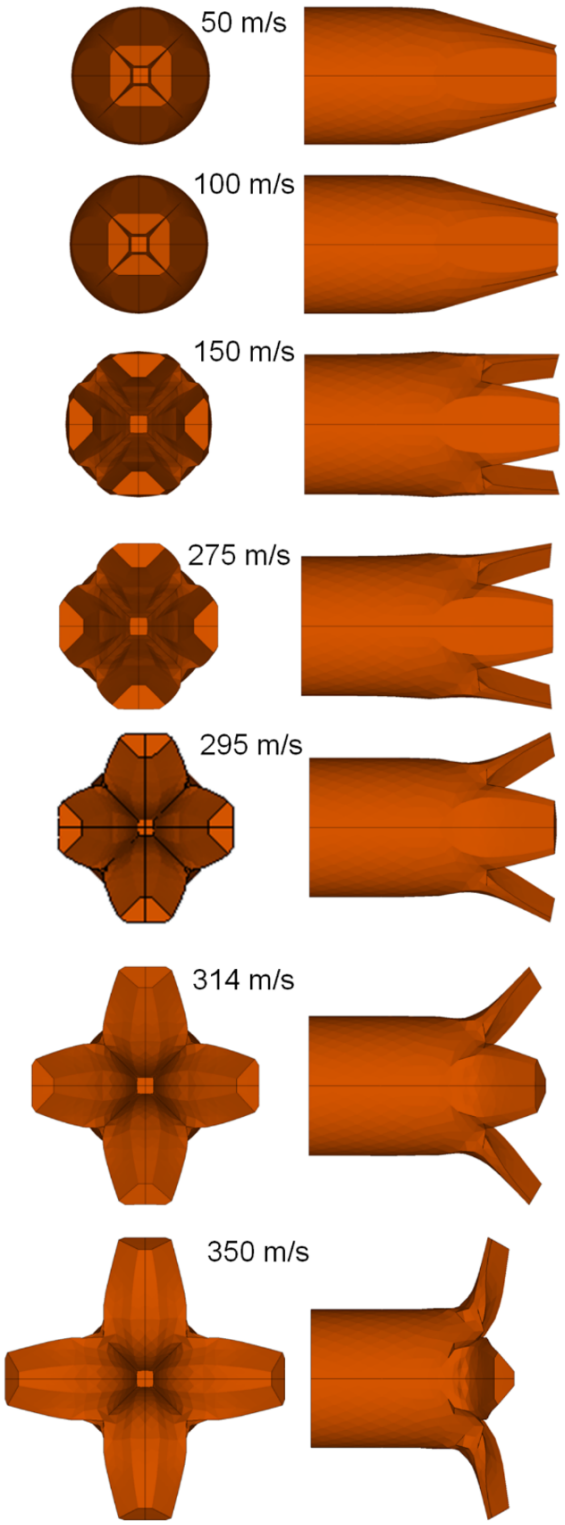

Fig. 15. Final deformations of bullets for different impact velocities

impact velocity increase up to a value of 250 m/s, a greater distance is achieved by bullets. However, with a further increase in V_i, it is observed that the time-distance dependence curve slopes down. Confronting the velocity curves with the images of final deformations of bullets, the reason for the change in the shape of curves can be found.

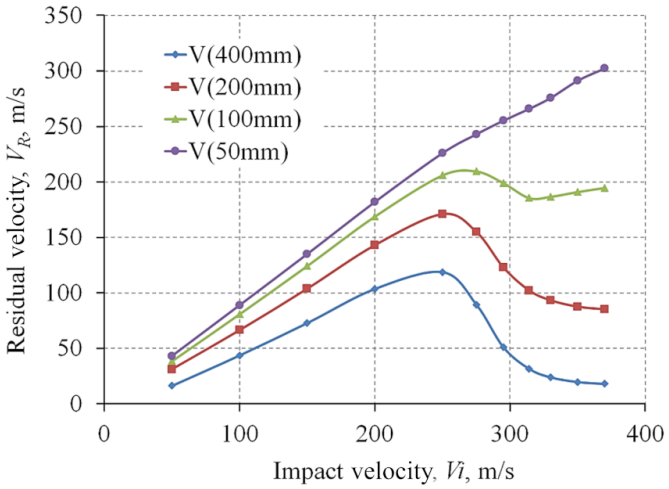

Fig. 16. Relationship between residual velocity and impact velocity for different distances

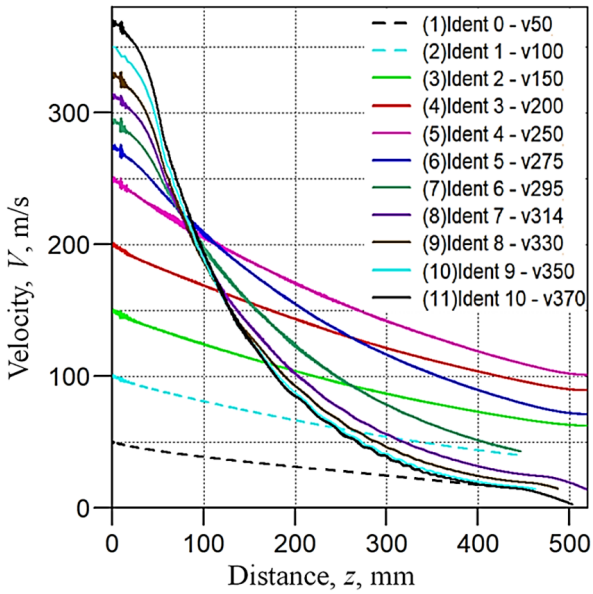

Fig. 17. Dependence of bullet velocity on distance

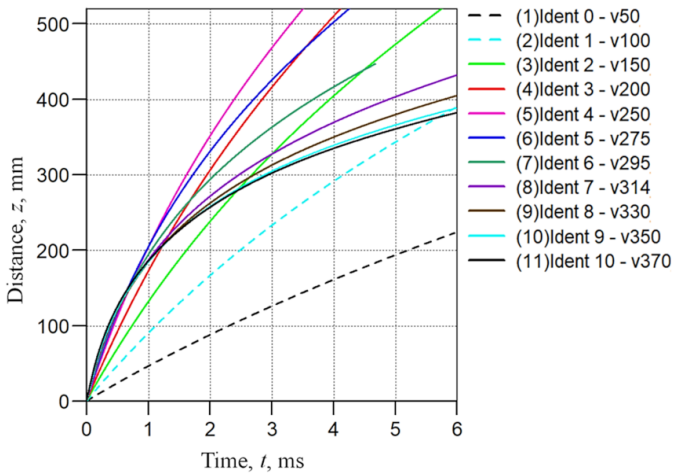

Fig. 18. Dependence of bullet velocity on distance

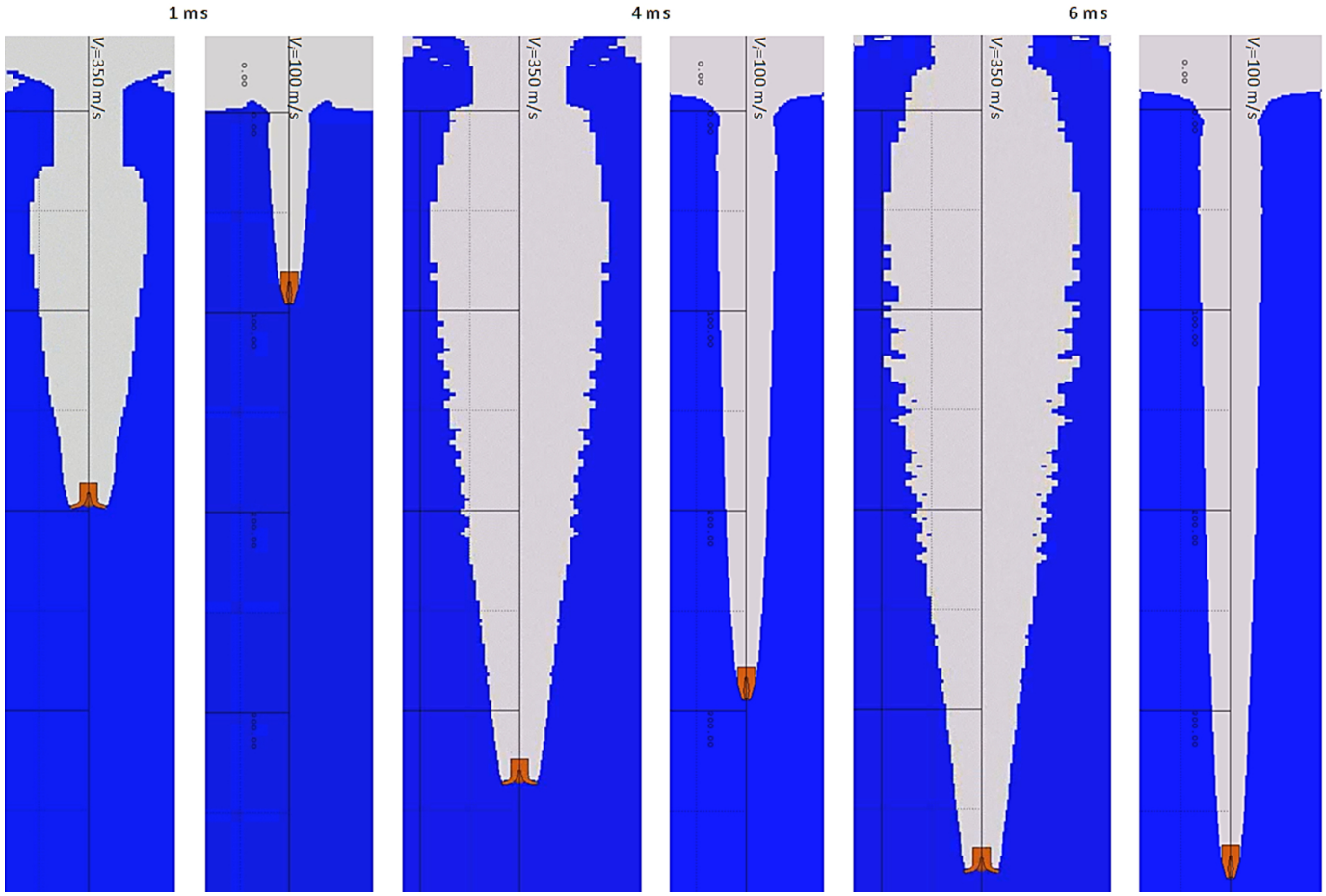

Fig. 19. Results of numerical simulations for velocities of bullet impact into water V_i = 100 m/s and 350 m/s

In the range of impact velocities 250–275 m/s the diameter of the deformed bullet resulting from the bending of the four petals at the front begins to exceed the diameter of the cylindrical part of the bullet. Consequently, this causes an increase in the resistance to motion and the rate of loss of bullet velocity. For example, after 6 ms, the bullets with impact velocities of 100 m/s and 350 m/s achieved approximately the same distance, 390 mm and 385 mm, respectively (Fig. 19). Moreover, for a 3.5 times smaller value of the impact velocity after these 6 ms, the residual velocity is more than doubled (Fig. 19). This is explained by the fact that for a higher impact velocity, the projectile opened, while for the lower it remained closed.

4.5. Results of ballistic tests on the composite system for the bullet catcher

In the last step, ballistic tests of two material configurations, with and without a composite structure, were performed using a bullet with nominal impact velocity. Plasticine was used as the medium placed behind the composite (Fig. 20). In the case of a 150 mm-thick block of standalone plasticine, a bullet was found in the rear part. Strong projectile deformations, greater than in the case of water, are visible. The angle between the open part and the cylindrical part is greater. For water, it was about 90°, whereas in this case it is nearly 135°. This confirms the correctness of the earlier assumption that if satisfactory results with plasticine are obtained, it is also certain that they will be obtained in water, which is a medium that causes less deformation.

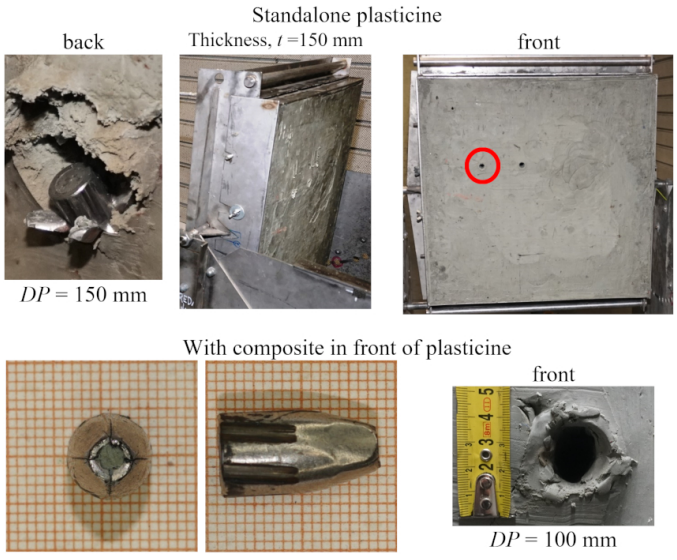

Fig. 20. Results of ballistic tests of 9 × 19 mm Geco Action Extreme bullet impact into ballistic plasticine with and without composite structure

In the other configuration, the composite structure that was developed was placed in the front of the plasticine. Thanks to this, the bullet was not deformed. The diameter and length remain the same as before the shot.

5. CONCLUSIONS

1. Methods used nowadays in forensic laboratories allow bullets to be stopped with a degree of deformation, which enables them to be used to compare traces to bullets found at a crime scene. However, they are not useful for all types of bullets, e.g., high-energy bullets susceptible to deformation.
2. With the use of the developed composite and plasticine, in the case of a monolithic hollow point 9 mm GECO Action Extreme bullet, it is possible to decelerate and slowly stop the bullet in a manner that does not cause its deformation.
3. Plasticine proved to cause greater bullet deformation than water. If satisfactory results can be obtained with plasticine in a material set with composite structure, it can be assumed that they would be obtained also in the case of the analogous system with water.
4. In the case of impact of a 9 mm GECO Action Extreme bullet into water, for distances greater than or equal to 200 mm, the residual velocity increases along with the increase in impact velocity up to a value of 250 m/s. In the case of higher impact velocities, a decrease in the residual velocity occurs.
5. The highest possible velocity for which deformation of a 9 mm GECO Action Extreme bullet is acceptable, the critical velocity V_{cr}, when no deformations are assumed, is within the range of 100–150 m/s.

ACKNOWLEDGEMENTS

This research was funded by Narodowe Centrum Badań i Rozwoju (The National Center for Research and Development), for the benefit of state defense and security (financing agreement number: DOB-BIO10/04/02/2019), title of the project: "Laboratory stand for stopping high-energy projectiles" with the acronym "Bullet Catcher". The project is implemented by the consortium: The Warsaw University of Technology – leader, Military Institute of Armament Technology, "Tebbex2" Centre of Shooting Technology.

REFERENCES

[1] J. Hansen, W. Piehl, and H. Plude, *A Method for Retrieving Fired Projectiles During the Data Acquisition Test*, General Thomas J. Rodman Laboratory Technical Report, Rock Island Arsenal, Rock Island, IL, USA, 1976.

[2] D. Lambert, M. Pope, S. Jones, and J. Muse, "Soft-recovery of explosively formed penetrators," *Conference Paper Preprint*, Air Force Research Laboratory, Eglin AFB, FL, USA, 2005. [Online]. Available at: https://apps.dtic.mil/sti/citations/ADA439174

[3] E. John, D. Bassett, Ch. Ream, M. Long, and N. Raisor, "Bullet catcher", EP Patent 2416103A2, 2012.

[4] E.V. Clarke, C.R. Ruth, J.W. Evans, J.E. Bowen, and J.R. Hewitt, *Large Caliber Projectile Soft Recovery*, Memorandum Report, US Army Armament Research and Development Command, Aberdeen Proving Ground, MD, USA, 1981.

[5] R.R. Chusnutdinov, "Bullet catcher", RU Patent 2235964C1, 2004.

[6] K.E. Schuessler, "Hydrodynamic bullet catcher", US Patent 2813422, 1957.

[7] R.M. Keppinger and J.M. Garner, *Soft Recovery of the M855 Bullet*, Final Report, Army Research Laboratory, Aberdeen Proving Ground, MD, USA, 2010.

[8] I. Yoo, S. Lee, and Ch. Cho, "Design study of a small scale soft recovery system," *J. Mech. Sci. Technol.*, vol. 20, no. 11, pp. 1961–1971, 2006, doi: 10.1007/BF03027589.

[9] E.B. Shaulsky, V.A. Grishin, and R.K. Umyarov, "Technical aids set of bullet catcher", RU Patent 2616291C1, 2017.

[10] L.P. Duke and E. Hart, "Polymeric ballistic material and method of making", US Patent 20060013977A1, 2006.

[11] L.P. Duke and W. Barrett, "Polymeric compositions for use in preparing a ballistic material", US Patent 20100173117A1, 2010.

[12] R.A. Mann, Ch. H. Slsk, and J.M. Natoli, "Bullet test tube and method", US Patent 7421893B1, 2008.

[13] F. Qing and M. Lei, "High-velocity projectile take-back device", CN Patent 104267204A, 2015.

[14] G. Jingwei, W. Jianhua, W. Jinglu, M. Debin, J. Chan, and Z. Huimin, "Portable gun speed measuring bullet collection device", CN Patent 201438093U, 2010.

[15] G. Johnson and W.A. Cook, "A constitutive model and data for metals subjected to large strains, high strain rates and high temperatures", in *Proc. 7th Int. Symp. Ballistics*, The Hague, Netherlands, 1983, pp. 541–547.

[16] A. Wiśniewski and D. Pacek, "Walidacja modelu numerycznego pocisku 9 mm Parabellum (Validation of the numerical model of the 9 mm Parabellum projectile)," *Mechanik*, vol. 2, pp. 138–140, 2012.

[17] A. Wiśniewski and D. Pacek, "Flexible modular armour for protection against the 5.56×45 mm SS109 projectiles," *Probl. Mechatron. Armament Aviat. Saf. Eng.*, vol. 6, pp. 21–40, 2015, doi: 10.5604/20815891.1157772.

[18] P. Badurowicz and D. Pacek, "Determining ricocheting projectiles' temperature using numerical and experimental approaches," *Materials*, vol. 15, p. 928, 2022, doi: 10.3390/ma15030928.

[19] G.R. Johnson and W.H. Cook, "Fracture characteristics of three metals subjected to various strains, strain rates, temperatures, and pressures," *Eng. Fract. Mech.*, vol. 21, no. 1, pp. 31–48, 1985, doi: 10.1016/0013-7944(85)90052-9.

[20] W. Burian *et al.*, "Protection effectiveness of perforated plates made of high strength steel", *Int. J. Impact Eng.*, vol. 126, pp. 27–39, 2019, doi: 10.1016/j.ijimpeng.2018.12.006.

[21] T. Fras, C.C. Roth, and D. Mohr, "Dynamic perforation of ultra-hard high-strength armor steel: Impact experiments and modelling", *Int. J. Impact Eng.*, vol. 131, pp. 256–271, 2019, doi: 10.1016/j.ijimpeng.2019.05.008.

[22] W. Chen and B. Song. *Split Hopkinson (Kolsky) Bar: Design, Testing and Applications*. Springer, 2011, doi: 10.1007/978-1-4419-7982-7.

[23] P. Zochowski *et al.*, "Finite element modelling of ballistic inserts containing aramid fabrics under projectile impact conditions – Comparison of methods", *Compos. Struct.*, vol. 294, p. 115752, 2022, doi: 10.1016/j.compstruct.2022.115752.

[24] H. Kolsky, "An investigation of mechanical properties of materials at very high rates of loading", *Proc. Phys. Soc. Lond.*, vol. B-62, pp. 676–700, 1949.

[25] R. Panowicz and J. Janiszewski, "Tensile split Hopkinson bar technique: Numerical analysis of the problem of wave disturbance and specimen geometry selection", *Metrol. Meas. Syst.*, vol. 23, pp. 425–436, 2016, doi: 10.1515/mms-2016-0027.

[26] P. Baranowski *et al.*, "Numerical study for determination of pulse shaping design variables in SHPB apparatus", *Bull. Pol. Acad. Sci. Tech. Sci.*, vol. 61, pp. 459–466, 2013, doi: 10.2478/bpasts-2013-0045.

[27] R. Othman, Ed., *The Kolsky-Hopkinson Bar Machine: Selected Topics*. Springer, 2018.

[28] P. Baranowski *et al.*, "Split Hopkinson pressure bar impulse experimental measurement with numerical validation," *Metrol. Meas. Syst.*, vol. 21, no. 1, pp. 47–58, 2014, doi: 10.2478/mms-2014-0005.

[29] J.R. Klepaczko, *Introduction to Experimental Techniques for Materials Testing at High Strain Rates*. Warsaw, Poland: Inst. of Aviation Sci. Lib., 2007.

[30] B.A. Gamma, "Split Hopkinson Pressure Bar Technique: Experiments, Analysis, and Applications", Ph.D. thesis, University of Delaware, Departement of Material Science and Engineering, USA, 2004.

[31] G.T. Gray, "Classic split-Hopkinson pressure bar testing", in *ASM Handb. Mech. Test. Eval.*, vol. 8, pp. 462–476, 2000, doi: 10.31399/ asm.hb.v08.a0003296.

[32] L. Kruszka, M. Magier and M. Zielenkiewicz, "Experimental analysis of visco-plastic properties of the aluminum and tungsten alloys by means of Hopkinson bars technique", *Appl. Mech. Mater.*, vol. 556, pp. 110–115, 2014, doi: 10.4028/www.scientific.net/AMM.566.110.

[33] L. Kruszka and M. Magier, "Experimental investigations of visco-plastic properties of the aluminum and tungsten alloys used in KE projectiles," *Eur. Phys. J. Web Conf.*, vol. 26, p. 05005, 2012, doi: 10.1051/epjconf/20122605005.

[34] *Autodyn – Theory Manual*, Revision 4.3, Century Dynamics Inc., 2003.